






Article

LC-MS and GC-MS Data Fusion Metabolomics Profiling Coupled with Multivariate Analysis for the Discrimination of Different Parts of Fastrime Fruit and Evaluation of Their Antioxidant Activity

Ciro Cannavacciuolo ¹, Stefania Pagliari ¹, Chiara Maria Giustra ¹, Sonia Carabetta ², Werther Guidi Nissim ^{1,3}, Mariateresa Russo ², Paola Branduardi ^{1,3}, Massimo Labra ^{1,3,*}, and Luca Campone ^{1,3,*}

¹ Department of Biotechnology and Biosciences, University of Milano-Bicocca, Piazza Della Scienza 2, 20126 Milan, Italy

² Department of Agriculture Science, Food Chemistry, Safety and Sensoromic Laboratory (FoCuSS Lab), University of Reggio Calabria, Via dell'Università, 25, 89124 Reggio Calabria, Italy

³ NBFC, National Biodiversity Future Center, 90133 Palermo, Italy

* Correspondence: massimo.labra@unimib.it (M.L.); luca.campono@unimib.it (L.C.)

Abstract: The comparative chemical composition of different part of Fastrime fruits (peels, pulp, albedo, and seeds) extracted with different solvents was determined by GC-MS and UHPLC-HRMS QToF. The obtained data were also combined for their in vitro antioxidant activity by multivariate analysis to define a complex fingerprint of the fruit. The principal component analysis model showed the significant occurrence of volatile organic compounds as α -bisabolol and α -trans-bergamotol in the pulp and albedo, hexanoic acid in the seeds, and several coumarins and phenolics in the peels. The higher radical scavenging activity of the pulp was related to the incidence of citric acid in partial least square regression.

Keywords: antioxidants; *Citrus australasica*; novel foods; polyphenols; foodomics; multivariate data analysis; principal component analysis



Citation: Cannavacciuolo, C.; Pagliari, S.; Giustra, C.M.; Carabetta, S.; Guidi Nissim, W.; Russo, M.; Branduardi, P.; Labra, M.; Campone, L. LC-MS and GC-MS Data Fusion Metabolomics Profiling Coupled with Multivariate Analysis for the Discrimination of Different Parts of Fastrime Fruit and Evaluation of Their Antioxidant Activity.

Antioxidants **2023**, *12*, 565. <https://doi.org/10.3390/antiox12030565>

Academic Editor: Volker Böhm

Received: 31 January 2023

Revised: 17 February 2023

Accepted: 21 February 2023

Published: 24 February 2023



Copyright: © 2023 by the authors. Licensee MDPI, Basel, Switzerland. This article is an open access article distributed under the terms and conditions of the Creative Commons Attribution (CC BY) license (<https://creativecommons.org/licenses/by/4.0/>).

1. Introduction

Citrus is a genus belonging to the Rutaceae family, which is widespread in tropical areas of the world. Several species are largely consumed as traditional food and studied for their content of phytochemicals, such as polyphenolics, coumarins, limonoids, and volatile organic compounds (VOCs), which confer bitterness and fresh aroma to the fruits. Growing attention in nouvelle cuisine is drawn to “finger limes” (*Microcitrus australasica*), also known as “citrus caviar” for the appealing praline pulp. The species originated from Queensland and New South Wales rainforests where seven different varieties were classified by the Australian cultivar registration authority [1]. The native fruits’ phenotype is different in the color of pulp and peels, but a unique composition in limonene/isomenthone/citronellal was assessed as chemical volatile markers for the genus [2]. The large request for novel foods characterized by innovative flavor, texture, and appearance, is responsible for the extended production of finger limes in other regions of the world. In particular, the temperate climate and sunny weather of the Mediterranean area shows ideal environment conditions for growing the Fastrime cultivar, a hybrid of *Fortunella* spp., *Microcitrus australasica*, and *Citrus aurantifolia* [3,4]. The ripe fruit, harvested from July to November, appears with a vivid green peel and white pulp. The caviar-like pulp is captivating in gourmet cuisine to garnish fish or meat or beverages, releasing a pungent aroma and citric taste with a hint of pepper. The peels are used as a fresh spice to flavor dishes, while other parts (seeds and albedo) are usually discharged despite the high price of

the fruit. The distinctive aroma of the fruit could be determined by the unusual volatile constituents in *Citrus*, such as limonene, β -phellandrene, and γ -terpinene, as reported in the Faustrime cultivar from Sicily [5]. Moreover, the occurrence of citronellal is reported as a major compound along with limonene, β -phellandrene, and γ -terpinene in a cultivar from southern Italy [3].

Polyphenols as flavonoids usually described in *Citrus* are reported for their antioxidant activity [6], cancer prevention [7], and metabolic syndrome alleviation [8]. Among the more than 170 molecules identified in *Citrus* with biological activity, Faustrime differed in the occurrence of eriocitrin, neoeriocitrin, diosmin, and neodiosmin content [9] without conferring a qualitative relevance between peel and pulp. Limonoids are oxygenated terpenoid compounds with several pharmacological properties, including anticancer, antimicrobial, and antidiabetic activity. This interesting class of bioactive compounds typically occurs in the peel, albedo, or seeds, conferring bitterness to the fruits [10,11]. Among triterpenoids, only limononic acid was previously reported in the Faustrime cultivar [9]. Coumarins and furanocoumarins represent a consistent family of benzopyrone compounds commonly investigated in *Citrus*. Despite the assumption that pure coumarin could be hepatotoxic, coumarins naturally occurring in foods are allowed according to the new European aroma law [12] and studied for their anticancer activity [13]. Faustrime fruits are considered a high-value foodstuff for the growing gastronomic demand and healthy potential. Despite the large diffusion in cultivation crop and consumption of the fruit, specific studies reporting the metabolomic description of VOCs and secondary metabolites (polyphenols, coumarins, terpenes) are still lacking.

In line with the increasing demand for health-promoting products, several tools are largely used to describe the occurrence of bioactive phytochemicals in foods. Foodomics is an innovative approach to investigate functional foods integrating complex data from chemical identification such as mass spectrometry profiling and biological response [14]. In the current study, a comprehensive quali-quantitative investigation of VOCs and non-volatile compounds in Faustrime fruit was provided by means of GC-MS and UHPLC-QTOF-MS/HRMS analyses. The characterized chloroform and hydroalcoholic extracts, obtained from different parts of the fruit: peel (PE), pulp (PU), albedo (AL), and seeds (SE), were tested for antioxidant activity by measuring DPPH \bullet and ABTS \bullet^{+} radical scavenging capacity. Finally, imaging techniques were used for the comprehensive fingerprint of the fruit by multivariate data analysis such as principal component analysis (PCA) and partial least square regression (PLS) to observe the fruit's metabolomics and the chemical correlation with antioxidant activity.

2. Materials and Methods

2.1. Chemicals and Reagents

Analytical-grade methanol and n-hexane for extractions were obtained from Sigma-Aldrich (Milan, Italy). Ultrapure water (18 M Ω) was prepared by a Milli-Q purification system (Millipore, Bedford, MA, USA). methanol (MeOH), water, and formic acid with LC-MS grade were supplied by Romil (Cambridge, UK). Reference standards (>98% HPLC grade) apigenin, luteolin, rutin, coumarin, eriocitrin, isorhamnetin, hesperetin, naringenin, 1,1-diphenyl-2-picrylhydrazyl (DPPH \bullet), and 2,2-azinobis-(3-ethylbenzothiazoline-6-sulfonate) (ABTS \bullet^{+}) reagents were purchased from Sigma-Aldrich (Milan, Italy). Standard stock solutions (1 mg mL $^{-1}$) of each compound were prepared in methanol and stored at 4 °C. Diluted solutions and standard mixtures were prepared in MeOH/H $_2$ O:2:8 (v/v).

2.2. Plant Material and Extracts Preparation

The Faustrime fresh fruits (1 kg) were harvested in the ripening stage in the Napoli province of Italy (40.7085; 14.5258) in October 2022. All parts of the fresh fruits were manually separated and extracted with n-hexane (solid-liquid ratio 1:20 w/v) at room temperature for 2 nights for the extraction of volatile organic compounds (VOCs), as reported by Guzowska et al., 2022 [15]. For the recovery of the non-volatile compounds, PE, PU,

AL, and SE were freeze-dried, pulverized, and extracted with chloroform via maceration (solid–liquid ratio 1:20 *w/v*) for 3 nights, 3 times for each solvent [16]. Subsequently, a mixture of methanol/water 50% (*v/v*) was used for recovery of polar fraction using the same extraction conditions reported above. The *n*-hexane extract was dried under nitrogen flow while chloroform and hydroalcoholic extracts were dried under a rotatory vacuum evaporator and stored at +4 °C, protected from light until analysis.

2.3. Semi-Quantitative GC-MS Analysis

The volatile composition of *n*-hexane extracts was investigated by gas chromatography–mass spectrometry (GC-MS_QP2010 Ultra-Shimadzu, Milan-Italy). Volatile compounds were separated using a capillary column MEGA SE52 (5% Phenyl, 95% Methyl Polysiloxane 30 m × 0.25 mm i.d., 0.25 µm film thickness, MEGA s.r.l, Milan, Italy). The oven temperature was held at 40 °C for 3 min and then increased at 6 °C/min to 200 °C and then increased at 15 °C/min to 250 °C for 5 min. The total run time was 38 min. The carrier gas was helium (purity > 99.999%). The injection temperature was set to 270 °C; the injection mode was split with a split ratio of 50. The mass scan spectra were recorded from 35–500 amu with the electron ionization (EI) source set to 70 eV. The MS ion source and interface temperature were set to 280 °C, and a solvent cut time of 0.5 min was selected. GCMS SOLUTION software (Shimadzu, Milan, Italy) was used for the control of equipment and data acquisition. The relative abundance (%) was calculated by dividing the area of each individual peak by the total sum of all detected peak areas multiplied by 100. Compound identification was made by comparing mass spectra with NIST11 library data.

2.4. Qualitative and Semi-Quantitative Analysis by UPLC-ESI/HRMS-UV

Qualitative and quantitative analyses of chloroform extracts and hydroalcoholic extracts were performed by using a system of liquid chromatography coupled with electrospray ionization (ESI) and high-resolution mass spectrometry (UPLC-ESI/HRMS), a Waters ACQUITY UPLC system coupled with a Waters Xevo G2-XS QToF Mass Spectrometer (Waters Corp., Milford, MA, USA), operating in both negative and positive ionization modes. The chromatographic separation of chloroform extracts was performed on a Biphenyl column (100 mm × 2.1 mm, 2.6 µm; Phenomenex, Torrance, CA, USA) held at 30 °C by using a mobile phase consisting of 0.1% (*v/v*) formic acid in water as solvent A and 0.1% (*v/v*) formic acid in acetonitrile as solvent B, a flow rate of 0.4 mL min^{−1}, and a linear gradient from 0 to 20.0 min held in a range of 30–80% of the organic phase (B); from 20.0 to 25.0 min rising to 90% B; from 25.0 to 30.0 min rising to 95% B; 3 min of column washing (95% B) and 5 min of column equilibration at 30% B was performed before the next sample injection. For the chromatographic separation of hydroalcoholic extracts, a linear gradient from 5–10% B in 2 min, rising to 80% B in 17 min, rising to 95% B in 18 min; after each run, 3 min of column washing (95% B) and 5 min of column equilibration (5% B) was used. The autosampler was set to inject 5 µL of each extract at a concentration of 0.5 mg mL^{−1}. For the ESI source, the following experimental conditions were used: electrospray capillary voltage 2.5 kV, source temperature of 150 °C, and desolvation temperature of 500 °C. MS spectra were acquired by full range acquisition covering a mass range from 50 to 1200 *m/z*. The MS/HRMS analysis was provided by data-dependent scan (DDA). Experiments were performed by selecting the first and the second most intense ions from the HRMS scan event and submitting them to collision-induced dissociation (CID) by applying the following conditions: a minimum signal threshold at 250, an isolation width at 2.0, and normalized collision energy at 30%. Both in full and in MS/HRMS scan mode, a resolving power of 30,000 was used. Compound deconvolution was attributed via MS-DIAL 4.90 open-source software comparing MS/HRMS spectra with “ESI(-)-MS/HRMS from authentic standards (9033 unique compounds)” library data and confirmation with literature reports.

For semi-quantitative analysis, stock solutions (1 mg mL^{−1}) of each used compound as external standards were prepared by dissolving each compound in a solution of methanol. Increasing solution concentrations (0.1, 0.5, 1, 5, 10, and 50 µg mL^{−1}) were prepared for

the calibration curve construction by UHPLC-UV, wavelength set at 280 nm. In particular, 5 μL of each standard solution at each concentration was injected in a technical triplicate. Calibration curves were obtained by using linear regression using the Excel 2016 Software (Microsoft Corporation, Washington, DC, USA), considering the area of external standards against the known concentration of each compound. The obtained calibration curves showed good linearity (with correlation coefficients (R^2) ranging from 0.9969 to 0.9999, respectively, and all information is provided in supplementary material (Table S1). The quantitative data are expressed as mg g^{-1} of dried extract (EXT). The MassLynx software version 4.2 (Waters, Wilmslow, UK) was used for instrument control, data acquisition, and processing.

2.5. Determination of DPPH and ABTS Radical Scavenging Activity

The free radical scavenging activities of extracts were determined using the 1,1-diphenyl-2-picrylhydrazyl radical (DPPH \bullet) and 2,2-azinobis-(3-ethylbenzothiazoline-6-sulfonate radical cation) (ABTS \bullet^+) by the slightly modified methods previously described [17,18]. For the determination of DPPH \bullet scavenging activity, an aliquot (50 μL) of the extract (1 mg mL^{-1}) or standard solution (2.5–10 $\mu\text{g mL}^{-1}$) was added to 950 μL of prepared radical solution (0.14 mM). After darkness incubation for 30 min at room temperature, samples were read by spectrophotometer at a wavelength of 515 nm. For the ABTS \bullet^+ scavenging activity, the reaction was initiated by the addition of 50 μL of extract in 950 μL of diluted ABTS (14 mM) of each sample solution. The spectrophotometer was set with a wavelength of 734 nm. Determinations were repeated three times. The absorbance was calculated for each concentration relative to a blank absorbance (methanol) and was plotted as a function of the concentration of compound or standard, 6-hydroxy-2,5,7,8-tetramethylchroman-2-carboxylic acid (Trolox). The antioxidant activity was expressed as Trolox equivalents (TE) value representing the μmol of a standard Trolox solution exerting the same antioxidant capacity as 1 mg mL^{-1} of the tested extract.

2.6. Data Fusion Approach and Multivariate Data Analysis

A large dataset containing GC-MS and UPLC-MS data of all investigated compounds was organized for multivariate data analysis with a 'Low-level' data fusion approach [19]. The GC-MS matrix was made by 59 variables (metabolites tentatively identified in *n*-hexane extracts) and 4 observations (PE, PU, AL, and SE), while the LC-MS matrix contained 35 variables for the metabolites tentatively identified in chloroform and hydroalcoholic extracts of the same observations. To observe the comprehensive distribution of the volatile and polar compounds in four selected parts, the integrations of GC-MS and LC-MS signals were selected in the matrices and normalized by average function to balance the areas under the curve (AUC) obtained by the two tools. Finally, the total matrix was described by 94 variables (metabolites tentatively identified by GC-MS and LC-MS analysis) and 4 observations (PE, PU, AL, and SE). The obtained dataset was imported into SIMCA $^{\text{®}}$ (Sartorius, Goettingen, Germany) 17 for statistical analysis and modeling of score and loading plots. PCA and PLS models were described by two main principal components, scaled by Pareto mode and Autofit function. For reproducibility of the analysis, three extraction replicates and three replicate injections per sample extract were provided. LC-MS and GC-MS experiments were randomized; several injections of extraction solvent (blank) and a mix of all the samples (QC) were periodically injected for each five-acquisition analysis. The injection of QC ensures the reproducibility and stability of the MS signals during the acquisition batch and also guarantees the robustness of the chemometric results.

2.7. Statistical Analysis

Each GC-MS and LC-MS experiment was performed in triplicate. The variance in assessing differences between groups was evaluated by one-way ANOVA (considered to be significant at $p \leq 0.05$) on Microsoft Excel 2016. DPPH \bullet and ABTS \bullet^+ radical scavenging tests were carried out in triplicate and the results were expressed as mean \pm standard

deviation (SD). Multivariate data analysis was performed by principal component analysis (PCA) and partial least square (PLS) imaging techniques operating the linear regressions on the mean-scaled dataset to select the two main principal components. The choice of principal components was established based on the fitting (R^2X , 0.623) and predictive (Q^2X , 0.078) values. For PCA models, the chosen PC1 and PC2 explained 62.3% and 22.6% of the variance, respectively, for a total explained variance of 84.9%. The PLS analysis showed a distinct separation (R^2Y , 0.702) and good predictability (Q^2 , 0.365). No outliers were detected based on Hotelling's T^2 and Q residual statistical test (confidence level of 95%).

3. Results and Discussion

3.1. Composition of Volatile Organic Compounds in Faustrime Fruits

The profiles of *n*-hexane extracts of PE, PU, AL, and SE are reported in the supplementary material (Figure S1) and are described in detail in Table 1. Overall, 59 VOCs were identified and the relative abundance for each compound was reported. Monoterpenes were the most abundant VOCs identified, followed by sesquiterpenes. Generally, a citronellal/limonene/linalyl acetate chemotype can be considered for the investigated cultivar, highlighting differences in abundance ratios with previous studies [5,9]. The occurrence of linalyl acetate was reported for the first time in Faustrime. Significant differences in VOCs occurring in the four parts of the fruit were investigated in detail. The peel was the part of the fruit highlighting a larger number of GC-MS signals. In particular, citronellal was the most relative abundant monoterpene hydrocarbon detected in the peel (23.47%), followed by limonene, citronellol, and linalyl acetate (12.99%, 10.65%, and 7.65% respectively). An inverse citronellal/limonene ratio was registered for the peel of the investigated cultivar compared to the studies reported in the literature [5,8]. Differently, the pulp of the fruit highlighted the main content of linalyl acetate and limonene (18.23% and 11.40%, respectively), along with a higher content of *trans*-piperitol (1.83%) conferring the typical hint of paper to the culinary used pulp, compared to the peel, in contrast with Cioni et al., 2022 [9]. The detailed investigation of albedo and seeds of Faustrime was reported here for the first time. Linalyl acetate, citronellol, and limonene were the higher relative terpenes detected in the albedo (10.60%, 9.68%, and 9.03%, respectively) while cyclohexanol and hexanoic acid were mainly relative detected in the seeds (19.82% and 9.59%, respectively).

3.2. LC-HRMS Analysis of Faustrime Fruit

The chemical profiling of PE, PU, AL, and SE were investigated using UHPLC-(ESI)-DAD-MS/HRMS experiments. The chromatographic profiles of the chloroform and hydroalcoholic extracts of the four parts showed some differences, as reported in supplementary material (Figures S2 and S3).

The detailed identification of compounds was performed in several steps. Initial chemical deconvolution was performed by MS-DIAL software matching with the open access library provided by the website (<http://prime.psc.riken.jp/compsms/msdial/main.html>, accessed on 11 December 2022); then, identities were carefully confirmed by comparing the analyzed retention times, HRMS mass spectra, fragmentation patterns, and molecular formulas with the literature (Tables 2 and 3). Compounds 72–73, 80, 82, and 87 were confirmed based on the injection of reference standards. The following approach allowed the tentative identification of three coumarins and five furocoumarins reported for the first time in *Citrus australasica*; seven limonoids, despite only limonexic acid being previously reported in Faustrime [9]; and three organic acids. Moreover, six compounds related to the class of C-glycoside flavonoids, nine compounds ranked as O-glycoside flavonoids, and 2-hydroxymethylglutaryl flavonoids (HMG-flavones) were described, most of them reported for the first time in the specie.

Table 1. GC-MS VOCs detected in peel, pulp, albedo, and seeds of Faustrime fruit.

n. ^a	t _R	Compound	Relative Abundance (%)			
			Peel	Seed	Pulp	Albedo
1	8.79	β-phellandrene	0.18	-	0.06	0.08
2	8.85	β-pinene	0.07	-	0.16	0.10
3	9.36	β-myrcene	0.33	-	0.40	0.25
4	9.49	hexanoic acid	-	9.59	-	-
5	9.85	3-carene	0.10	-	0.14	0.09
6	10.27	ocymene	2.40	-	0.94	0.92
7	10.40	limonene	12.99	8.08	11.40	9.03
8	10.70	<i>trans</i> -β-ocimene	0.32	-	0.14	0.12
9	10.98	β- <i>cis</i> -ocimene	0.09	-	0.06	0.03
10	11.12	melonal	0.06	-	-	-
11	11.25	γ-terpinene	3.73	-	1.75	1.34
12	11.49	<i>cis</i> -sabinene hydrate	0.08	-	-	0.14
13	11.67	1-octanol	-	-	0.17	0.12
14	11.70	nonanal	0.07	-	-	-
15	12.05	4-carene	0.14	-	-	0.08
16	12.23	pantolactone	-	6.70	-	-
17	12.43	β-linalool	3.11	-	3.73	1.42
18	12.44	nonanal	0.29	7.67	-	0.15
19	12.99	<i>trans</i> -p-2-menthen-1-ol	0.48	-	2.47	1.31
20	13.35	<i>cis</i> -p-mentha-2,8-dien-1-ol	-	-	0.28	0.31
21	13.51	<i>cis</i> -p-2-menthen-1-ol	0.46	-	1.67	0.88
22	13.62	isopulegol	0.31	-	0.47	0.46
23	13.88	citronellal	23.47	15.04	0.40	3.93
24	14.13	(+)-isomenthone	1.39	-	2.17	0.55
25	14.29	1-(1,2,3-trimethyl-cyclopent-2-enyl)-ethanone	0.26	-	-	0.27
26	14.47	terpinen-4-ol	0.72	-	5.07	1.70
27	14.85	α-terpineol	2.71	-	6.18	4.02
28	15.07	[1,1'-bicyclopentyl]-2-one	-	-	0.71	0.54
29	15.20	decanal	0.35	-	1.33	0.37
30	15.28	<i>trans</i> -piperitol	0.78	-	1.83	0.72
31	15.85	citronellol	10.65	7.67	8.60	9.68
32	16.10	<i>cis</i> -citral	1.15	-	-	-
33	16.45	linalyl acetate	7.65	14.62	18.23	10.60
34	16.83	<i>trans</i> -citral	1.74	-	1.68	0.46
35	17.15	7-Oxabicyclo[4.1.0]heptane, 1-methyl-4-(2-methyloxiranyl)	0.64	-	-	-
36	17.69	limonene epoxide	0.42	-	-	0.52
37	18.12	(R)-(+)-citronellic acid	2.62	-	-	1.02
38	18.44	cyclohexanol, 2-(2-hydroxy-2-propyl)-5-methyl-	4.46	19.82	-	-
39	18.62	α-limonene diepoxide	0.61	-	-	-
40	18.80	2,6-octadiene, 2,6-dimethyl-	0.91	-	0.81	-
41	18.96	8-hydroxymenthol	1.77	-	3.66	-
42	19.07	2,6-octadien-1-ol-3,7-dimethyl-acetate	0.57	10.81	-	9.33
43	19.44	<i>cis</i> -isogeraniol	0.26	-	-	-
44	20.39	caryophyllene	0.61	-	-	-
45	20.72	α-bergamotene	1.20	-	-	-
46	21.15	humulene	0.75	-	-	-
47	22.08	nerolidyl acetate	0.55	-	-	-
48	22.17	levomenol	0.27	-	-	-
49	22.30	β-Bisabolene	1.75	-	0.59	-
50	22.51	α- <i>trans</i> -bergamotol	-	-	0.45	-
51	22.81	(-)-spathulenol	0.83	-	-	-
52	24.15	hexadecane	0.16	-	-	-
53	24.49	caryophyllene oxide	-	-	0.66	-
54	25.37	ledol	-	-	1.14	-

Table 1. Cont.

n. ^a	t _R	Compound	Relative Abundance (%)			
			Peel	Seed	Pulp	Albedo
55	25.92	α-bisabolol	0.23	-	2.96	0.53
56	28.52	ficusin	0.48	-	0.48	0.52
57	28.70	phytol acetate	-	-	0.43	-
58	30.71	n-hexadecanoic acid	0.43	-	4.96	8.36
59	31.70	methoxsalen	0.55	-	-	-

^a compounds are listed in ascending order of retention time.

3.2.1. Identification of Coumarins and Furocoumarins

The coumarins detected in the chloroform extracts showed a good MS response in positive mode, and they generally exhibited a distinct fragment ion $[M-CO_2+H]^+$ from the fragmentation of pyran-2-one, which could be used as a diagnostic ion for the characterization of coumarins and furocoumarins [12] in the fruit, as in the case of the peaks 60–61 and 71 (Table 2). In the case of furocoumarins 62–66, fragment ions $[M-CH_3+H]^+$, $[M-2CH_3+H]^+$, and $[M-2CH_3-CO+H]^+$ occur in the MS/HRMS spectra, revealed by the neutral loss of 15 Da, 30 Da, or 58 Da, respectively (Table 2). To the best of our knowledge, the identified coumarins (compounds 60–66) were described for the first time in *Citrus australasica*.

3.2.2. Identification of Limonoids

Limonoids are a class of oxygenated triterpenoids widely reported in *Citrus*. To distinguish them from other types of *Citrus* components in MS analysis, limonoids showed a distinct elemental composition (26–28 carbons) and degree of unsaturation (11–12), as well as a prominent ion at m/z 161.0595 in the positive mode MS² spectra and m/z 159.0233 in negative mode MS² spectra, which could be used as diagnostic ions for the class [20]. In the present study, compounds 67–70 were tentatively assigned to limonin, obacunoic acid, methyl nominilate, and veprisone, respectively, investigated in chloroform extracts (Table 2). Moreover, compounds 92–95 were tentatively identified in hydroalcoholic extracts as limonexic acid, citrusin, limonin and isobacunoic acid, respectively (Table 3). Limonin was detected in both chloroform and hydroalcoholic extracts and unambiguously identified by the injection of reference standards. The occurrence of limonexic acid was previously reported for Fastrime fruits by Cioni et al., 2022 [9], while the other investigated limonoids were reported for the first time in the specie.

Table 2. LC-MS data for coumarins, furocoumarins, and limonoids detected in chloroform peel, pulp, albedo, and seed extracts of Fastrime fruit.

n.	t _R	[M+H] ⁺	Compound	Class	ppm	Formula	MS/HRMS	Ref
60	6.11	163.0408	4-hydroxycoumarin	coumarin	8.0	C ₉ H ₆ O ₃	119.0075; 87.0074	[21]
61	6.96	193.0512	scopoletin	coumarin	5.7	C ₁₀ H ₈ O ₄	178.0267; 149.0314 133.0293; 105.0336 175.0391; 147.0442	[22]
62	10.15	203.0344	bergaptol	furocoumarins	8.7	C ₁₁ H ₆ O ₄	131.0491; 119.0492 103.0542	[22]
63	10.55	203.0364	xanthotoxol	furocoumarins	8.9	C ₁₁ H ₆ O ₄	175.0418; 147.0443 131.0497; 129.0337	[22]
64	13.39	187.0406	psoralen	furocoumarins	5.9	C ₁₁ H ₆ O ₃	131.0497; 115.0545 103.1522	[23]
65	15.00	217.0515	xanthotoxin	furocoumarins	6.5	C ₁₂ H ₈ O ₄	202.0258; 161.0612 146.0359; 131.0497 118.0431	[23]

Table 2. Cont.

n.	t _R	[M+H] ⁺	Compound	Class	ppm	Formula	MS/HRMS	Ref
66	16.92	247.0605	isopimpinellin	furocoumarins	1.4	C ₁₃ H ₁₀ O ₅	232.0360; 217.0154 189.0186; 161.0249 425.1989; 367.1981	[24]
67	17.14	471.2038	limonin	limonoids	4.0	C ₂₆ H ₃ O ₈	213.0987; 161.0612 133.0641 455.2148; 427.2138	standard
68	17.64	473.5294	obacunoic acid	limonoids	0.8	C ₂₆ H ₃₂ O ₈	369.2047; 341.2100 243.1015; 187.0770 161.0586 529.2419; 487.2338	[20]
69	19.34	547.2559	methyl nomilate	limonoids	2.9	C ₂₉ H ₃₈ O ₁₀	469.2249; 369.2047 351.1956; 341.2100 187.0770; 175.0743 161.0612	[25]
70	20.22	487.2338	veprisone	limonoids	1.2	C ₂₇ H ₃₄ O ₈	369.2047; 215.1087 161.0586; 133.0647 135.0451; 133.0269	[26]
71	21.44	163.0408	umbelliferone	coumarin	8.0	C ₉ H ₆ O ₃	119.0143; 120.0209 107.0499; 105.0336	[27]

3.2.3. Identification of HMG-Hexoside and HMG-Flavonoids

The first chromatographic region of hydroalcoholic extracts, reported in supplementary material Figure S3, showed organic acids (compounds 72, 73 and 74). Citric acid and ascorbic acid were assigned to compounds 72 and 73, respectively, for the overlapping of retention time and HRMS spectra with standards. Compound 74 showed a deprotonated ion [M-H][−] at *m/z* 365.1440 and typical MS/HRMS signals of HMG-moiety as the product ion [M-144-H][−] at *m/z* 221.1025, along with the diagnostic residue at *m/z* 125.0255, confirming the identity of propyl HMG-hexoside [22]. The fragmentation patterns of compounds 89 and 91 regarded the structure of flavones with HMG moiety, confirmed by the characteristic neutral loss of 144 Da (C₆H₈O₄) and a diagnostic ion at *m/z* 125.02272 (HMG-H₂O) in the MS/HRMS spectra. In particular, compound 89 showed a [M-H][−] at *m/z* 651.1567 (C₂₉H₃₂O₁₇). The fragments [M-144-H][−] at *m/z* 507.1143 and [M-162-144-H][−] at *m/z* 345.0618 were observed in MS/HRMS spectra suggesting the presence of 3-hydroxy-3-methylglutaryl moiety attached to the glycosyl group and the aglycone tetrahydroxy-dimethoxyflavone. A similar MS² pattern was observed for compound 91, showing a HRMS deprotonated ion [M-H][−] at *m/z* 675.1843 (C₃₄H₃₈O₂₀) never found in the MS database and the literature. In detail, HRMS and MS² Spectra are shown in supplementary material Figure S4. The fragments [M-144-H][−] at *m/z* 621.1473, and [M-(2×144)-H][−] at *m/z* 477.1016 highlight the occurrence of two HMG residues on the glycosylated isorhamnetin (C₂₂H₂₂O₁₂) whose molecular formula was obtained by high-resolution MS² patterns. The high-resolution fragment at *m/z* 315.0488 [M-(2×144)-162-H][−] confirms the occurrence of isorhamnetin as an aglycon scaffold. To the best of our knowledge, the tentatively identified di-HMG-hexoside-flavone is observed for time and tentatively attributed to isorhamnetin-di-HMG-O-glycoside.

3.2.4. Identification of C-Glycoside Flavonoids

Compounds 75, 77, 78, 79, 81, and 86 are ranked in the classes of C-glycoside flavonoids for the typical MS² patterns, highlighting diagnostic losses of M-90, M-120, and M-150 Da from the cross-ring cleavage of C-sugar of [M-H][−] ions (Table 3). The occurrence of C-glycoside flavonoids lucenin 2 (75), homoorientin (78), stellarin 2 (79), and scoparin (86) was reported for the first time in the species.

3.2.5. Identification of O-Glycoside Flavonoids

Differently, the compounds 76, 80, 82–85, 87–88, and 90 were characterized as O-glycoside flavonoids by the more favorable loss of glycoside units as dehydrated forms in the product ion spectra (Table 3). Fragments of $[M-162-H]^-$ and $[M-146-H]^-$ are commonly found for the presence of hexose and pentose sugars, respectively, while di-glycosides can also be detected with $[M-324-H]^-$ and $[M-308-H]^-$ fragments in the MS² pattern attributed to sucrose or rhamnose moieties, respectively. Rutin, neoeriocitrin, and naringenin 7-O-rutinoside were identified by the injection of standard, confirming the identification of neoeriocitrin for the first time in Faustrime.

Table 3. LC-MS data for organic acids, phenolic compounds, and limonoids detected in chloroform peel, pulp, albedo, and seed extracts of Faustrime fruit.

n.	tr	$[M-H]^-$	Compound	Class	ppm	Formula	MS/HRMS	Ref
72	1.04	191.0187	citric acid	organic acid	0.26	C ₆ H ₈ O ₇	111.0075; 87.0074	standard
73	2.51	175.1324	ascorbic acid	organic acid	1.32	C ₆ H ₈ O ₇	115.0043; 87.0043	standard
74	7.72	365.1440	propyl HMG-hexoside	organic acid hexoside	−2.2	C ₁₅ H ₂₆ O ₁₀	221.1020; 161.0461 125.0255; 113.0421 519.1135; 489.1046	[22]
75	8.38	609.1467	lucenin 2	C-di-glucosyl flavonoid	1.8	C ₂₇ H ₃₀ O ₁₆	429.0822; 399.0700 369.0594 519.1521; 477.1061	[28]
76	9.02	639.1581	isorhamnetin-3,7- di-O-glucoside	O-di-glucosyl flavonoid	1.3	C ₂₈ H ₃₂ O ₁₇	357.0322; 315.0561 473.1072; 383.0711	[29]
77	9.24	593.1518	vicenin 2	C-di-glucosyl flavonoid	2.1	C ₂₇ H ₃₀ O ₁₅	353.0654 399.0721; 357.0613	[29]
78	9.85	447.0903	homoorientin	C-glucosyl flavonoid	5.4	C ₂₁ H ₂₀ O ₁₁	327.0524; 299.0533 533.1282; 503.1197	[30]
79	10.57	623.1597	stellarin 2	C-di-glucosyl flavonoid	−2.4	C ₂₈ H ₃₂ O ₁₆	413.0865; 383.0760	[31]
80	10.87	609.1467	rutin	O-glucosyl-rhamnosyl flavonoid	1.8	C ₂₇ H ₃₀ O ₁₆	301.0337 341.0644; 323.0550	standard
81	11.07	431.0951	isovitexin	C-glucosyl flavonoid	3.5	C ₂₁ H ₂₀ O ₁₀	311.0563; 283.0600 459.1112;	[32]
82	11.34	595.1683	neoeriocitrin	O-glucosyl-rhamnosyl flavonoid	3.4	C ₂₇ H ₃₂ O ₁₅	287.0564 151.0007	standard
83	11.40	593.1581	luteolin-O- rutinoside	O-glucosyl-rhamnosyl flavonoid	2.0	C ₂₇ H ₃₀ O ₁₅	285.0374	[9]
84	12.15	623.1597	isorhamnetin-3-O- rutinoside	O-glucosyl-rhamnosyl flavonoid	−2.4	C ₂₈ H ₃₂ O ₁₆	315.0488	[33]

Table 3. Cont.

n.	tr	[M-H] ⁻	Compound	Class	ppm	Formula	MS/HRMS	Ref
85	12.30	477.1016	isorhamnetin-3-O-glucoside	O-glucosyl flavonoid	1.9	C ₂₂ H ₂₂ O ₁₂	357.0584; 314.0392 285.0490; 271.0228 243.0278; 151.0007 371.0762;	[33]
86	12.38	461.1097	scoparin	C-glucosyl flavonoid	2.2	C ₂₂ H ₂₂ O ₁₁	341.0644 298.0462	[34]
87	12.55	579.1719	naringenin-7-O-rutinoside	O-glucosyl-rhamnosyl flavonoid	0.9	C ₂₇ H ₃₂ O ₁₄	271.0599; 151.0032	standard
88	12.87	607.1673	diosmetin-7-O-rutinoside	O-glucosyl-rhamnosyl flavonoid	1.6	C ₂₈ H ₃₂ O ₁₅	299.0546; 284.0254 607.1673; 589.1590	[29]
89	13.16	651.1567	tetrahydroxy-dimethoxyflavone HMG-hexoside	HMG-hexoside-flavonoid	3.2	C ₂₉ H ₃₂ O ₁₇	549.1228; 507.1143 345.0618	[35]
90	13.58	609.1821	hesperetin-7-O-rutinoside	O-glucosyl-rhamnosyl flavonoid	0.3	C ₂₈ H ₃₄ O ₁₅	301.0639; 286.0824 621.1473;	[29]
91	13.99	765.1843	isorhamnetin-di-HMG-O-glycoside	di-HMG-hexoside-flavonoid	-4.1	C ₃₄ H ₃₈ O ₂₀	477.1016 315.0488; 125.0233 457.1872;	-
92	14.88	501.1788	limonexic acid	limonoid	-3.8	C ₂₆ H ₃₀ O ₁₀	413.1948 59.0214 501.2155; 457.2222	[22]
93	16.78	545.2000	citrusin	limonoid	-4.2	C ₂₈ H ₃₄ O ₁₁	397.1988; 373.2013; 125.0233; 59.0233	[22]
94	17.70	469.2869	limonin	limonoid	1.5	C ₂₆ H ₃₀ O ₈	451.1738; 249.1307 229.1233; 59.0232	standard
95	17.78	471.2027	isoobacunoic acid	limonoid	1.7	C ₂₆ H ₃₂ O ₈	453.1898; 261.1464 231.0988; 59.0342	[22]

3.3. Semi-Quantitative Analysis of Coumarins and Flavonoids

Qualitative analysis was combined with a semi-quantitative approach to highlight the different distribution of secondary metabolites among the different parts of the matrix. Semi-quantitative analysis was performed using a UPLC-UV at a wavelength of 280 nm, and quantification was carried out by using calibration curves in a range of 0.1–50 µg mL⁻¹ with 8 standards, reported in Table S1, used for the classification of all major phenolic compounds and coumarins. Compounds for which authentic standards were not available were quantified into standard equivalents using the most chemically related standard available.

The results of the semi-quantitative analysis (Table 4) showed the different amount distribution of coumarins and phenolics in PE, PU, AL, and SE, relatively. In detail, Faustrime PE showed the highest phenolic compounds and coumarin concentration. Among these, the highest relative amounts are referred to compounds 60, 62, 64, 76, 80, 87 and the

newly observed compound 91 (Table 4). In addition, the absence of coumarins was highlighted in the albedo portion compared to the peel and pulp, where they were found and quantified (compounds 60 to 66). However, neoeriocitrin prevailed in the albedo (10.92 mg/g EXT) compared to the other parts of the fruit, while diosmetin-7-*O*-rutinoside was mainly contained in the pulp (11.33 mg/g EXT). The UPLC-UV profile of the seeds did not show a considerable signal of non-volatile compounds for the quantification (Figure S3 supplementary material).

Table 4. Semi-quantitative analysis of non-volatile compounds.

N	Compounds	Peel *	Pulp *	Albedo *
Chloroform Extract				
60	4-hydroxycoumarin ^a	4.34 ± 0.25	1.78 ± 0.38	-
61	Scopoletin ^a	2.34 ± 0.38	-	-
62	Bergaptol ^a	9.63 ± 0.82	4.42 ± 0.25	-
63	Xanthotoxol ^a	5.34 ± 0.41	1.90 ± 0.18	-
64	Psoralen ^a	145.57 ± 9.65	6.95 ± 0.67	-
65	Xanthotoxin ^a	35.00 ± 1.85	8.17 ± 0.68	-
66	Isopimpinellin ^a	2.55 ± 0.14	1.54 ± 0.21	-
Hydroalcoholic Extract				
75	lucenin 2 ^b	10.78 ± 1.37	6.91 ± 0.38	6.92 ± 0.43
76	isorhamnetin-3,7-di- <i>O</i> -glucoside ^c	60.60 ± 4.62	9.77 ± 0.75	13.60 ± 0.87
77	vicenin 2 ^d	19.38 ± 2.15	3.94 ± 0.11	3.46 ± 0.15
78	homoorientin ^b	4.50 ± 0.98	1.83 ± 0.20	2.28 ± 0.29
79	stellarin 2 ^c	27.56 ± 2.05	12.06 ± 0.65	25.60 ± 1.08
80	rutin ^e	94.45 ± 5.13	52.17 ± 3.44	34.50 ± 2.12
81	isovitexin ^d	2.30 ± 0.13	1.36 ± 0.09	1.67 ± 0.14
82	neoeriocitrin ^f	9.32 ± 0.79	4.80 ± 0.32	10.92 ± 0.82
83	luteolin- <i>O</i> -rutinoside ^b	11.62 ± 0.99	6.77 ± 0.59	7.95 ± 0.71
84	isorhamnetin-3- <i>O</i> -rutinoside ^c	12.96 ± 0.81	10.55 ± 0.83	8.74 ± 0.52
85	isorhamnetin-3- <i>O</i> -glucoside ^c	11.32 ± 0.98	8.31 ± 0.79	10.25 ± 1.05
86	scoparin ^c	13.56 ± 0.85	9.67 ± 0.67	8.58 ± 0.96
87	naringenin-7- <i>O</i> -rutinoside ^g	25.86 ± 1.54	2.74 ± 0.13	3.63 ± 0.36
88	diosmetin-7- <i>O</i> -rutinoside ^c	7.34 ± 0.71	11.33 ± 1.03	7.41 ± 0.81
89	tetrahydroxy-dimethoxyflavone HMG-hexoside ^c	10.77 ± 0.89	5.11 ± 0.38	7.61 ± 0.77
90	hesperetin-7- <i>O</i> -rutinoside ^h	19.87 ± 1.11	5.07 ± 0.42	15.55 ± 1.28
91	isorhamnetin-di-HMG- <i>O</i> -glycoside ^c	38.18 ± 2.98	11.33 ± 0.95	6.75 ± 0.56

Calculated using the calibration curves of: ^a coumarin; ^b luteolin; ^c quercetin; ^d apigenin; ^e rutin; ^f eriocitrin; ^g naringenin, and ^h hesperetin. * data are expressed as mg std equivalent/g of dried extract (EXT).

3.4. Antioxidant Properties of Bioactive Containing Extracts

The comparison between chloroform and hydroalcoholic extracts of the different parts of the fruit (PE, PU, AL, and SE) to determine the antioxidant activity was performed by DPPH• and ABTS•⁺ assays. Generally, the hydroalcoholic extracts showed higher activity than chloroform extracts. In particular, the hydroalcoholic extracts of the pulp and albedo showed a higher capacity to neutralize both DPPH• and ABTS•⁺ radicals (Table 5). The peel showed a lower scavenging capacity with TE values of 2.75 ± 0.05 and 8.22 ± 0.32 for DPPH• and ABTS•⁺, respectively, whereas seeds showed very low antioxidant activities (Table 5).

Table 5. DPPH• and ABTS•+ radical scavenging capacity of hydroalcoholic and chloroform extracts.

Part	Extract	DPPH•	ABTS•+
		mean TE ± SD	mean TE ± SD
Peel	Hydroalcoholic	2.75 ± 0.05	8.22 ± 0.32
	Chloroform	2.06 ± 0.04	5.01 ± 0.11
Pulp	Hydroalcoholic	7.58 ± 0.12	10.51 ± 0.34
	Chloroform	1.73 ± 0.02	3.61 ± 0.11
Albedo	Hydroalcoholic	7.71 ± 0.32	10.82 ± 0.45
	Chloroform	1.15 ± 0.11	7.73 ± 0.26
Seeds	Hydroalcoholic	3.64 ± 0.23	4.19 ± 0.12
	Chloroform	3.07 ± 0.15	1.21 ± 0.09

mean TE values are expressed as µg of standard Trolox solution exerting the same radical scavenging activity of 1 mg/mL of the tested extract. SD is the standard deviation of three independent experiments.

3.5. Combined Multivariate Data Analysis by PCA and PLS

With the aim to visualize a complex set of chemical data and correlating the radical scavenging capacity to specific metabolites contained in the investigated extracts, a supervised multivariate data analysis was carried out. Specifically, a combined data analysis was performed by principal component analysis (PCA) and partial least squares–discriminant analysis (PLS-DA) methods to discriminate between the samples and model the complex metabolome of Faustrime.

Data fusion furnishes statistical results to obtain the maximum number of correctly classified samples by combining the data obtained from different instrumental techniques. One of the strategies is ‘low-level’ data fusion, where the two blocks of data (LC and GC matrices) obtained from the mass spectrometry techniques are pre-treated and mixed in a single dataset [36]. After a detailed targeted analysis of the GC-MS and LC-MS profiles of Faustrime’s VOCs and non-volatile compounds, in the second stage, the combination of the data from the different instruments by means of ‘low-level’ data fusion strategy was performed to build a comprehensive metabolomic fingerprint. The ‘low-level’ data fusion strategy consists of concatenating the individual LC-MS and GC-MS data matrices, opportunely pre-treated, and finally, concentrating the resulting data in a single block [19]. The different data matrices corresponding to the GC-MS profiles related to the *n*-hexane extracts of the four different parts of the fruit integrated with HPLC-MS profiles recorded for chloroform and hydroalcoholic extracts were concentrated using the mean-centering pre-treatment to normalize data obtained by different analytical tools [19].

The first principal component (PC1) divided the peel on the left part (PC1 < 0) of the PCA biplot and the group containing albedo, pulp, and seeds (PC1 > 0) on the right quadrant of the biplot (Figure 1A). In detail, the cluster of albedo and pulp was plotted on the upper right quadrant (PC1 > 0, PC2 > 0), discriminated for the content of several VOCs, such as α -bisabolol, 2-menthen-1-ol, and α -*trans*-bergamotol, while seeds laid on the opposite quadrant along the second principal component (PC1 > 0, PC2 < 0) for the incidence of hexanoic acid. The presence of all the identified non-volatile compounds and most of the VOCs resulted in the discrimination of the peel. The incidence of the metabolites on that cluster depended on their distance from the origin, highlighted in detail by the contribution bars of Figure 1B. Citronellal is the main constituent of volatile chemotype interfering in the peel discrimination, along with the detected HMG-flavonoids, lucenin 2, stellarin 2, and vicenin 2 C-glycoside flavonoids, scopoletin and psolarene (coumarin and furocoumarin, respectively) and caryophyllene, α -bergamotene (terpenes), mainly occurring in peels. PCA loading and PCA score plots are shown in Figures S5 and S6 of the supplementary material, respectively.

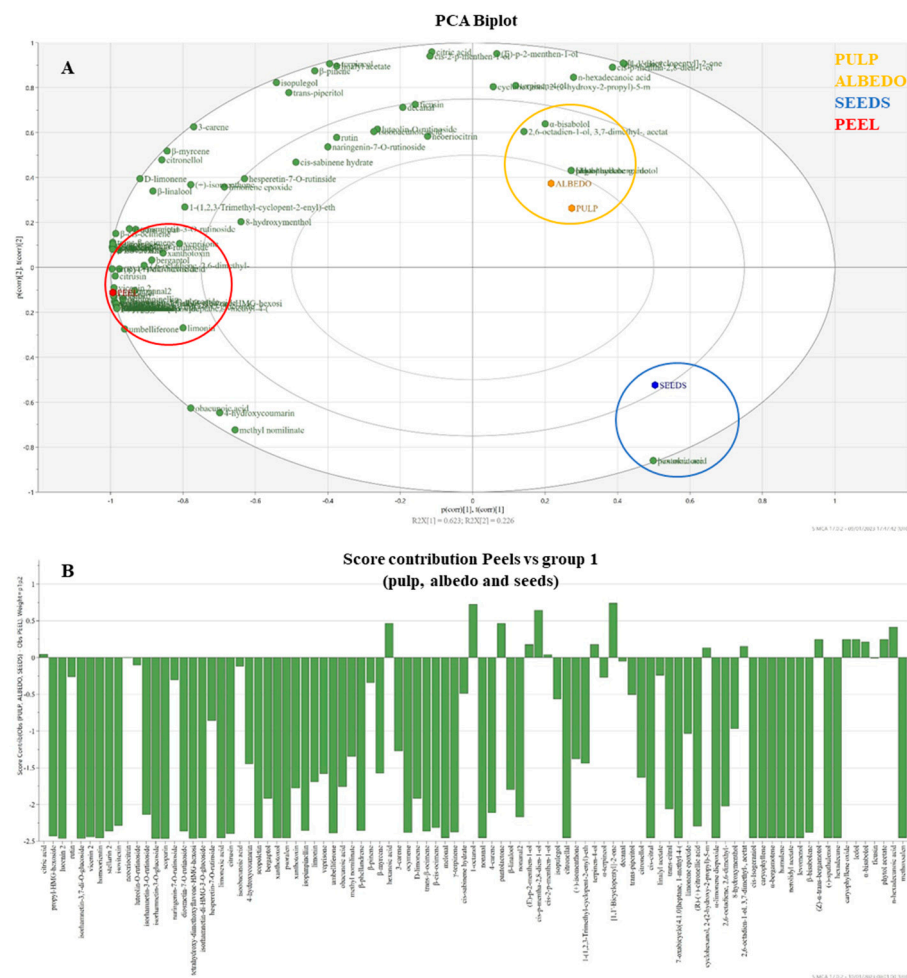


Figure 1. Biplot of PCA analysis performed on peels (red spot), pulp, albedo (yellow spot), and seeds (blue spot) for the identified VOCs and non-volatile compounds (A). Contribution diagram of the constituents on the distribution of samples (B).

Partial least square regression (PLS) was performed for the attribution of classes to the chloroform and hydroalcoholic extracts based on the different capacities to neutralize DPPH• and ABTS•+ radicals among the extracts of peel, pulp, and albedo. The seeds are not considered because of their low activity in the spectrophotometric tests. PLS showed the separation along the first principal component (PC1) between the peel (PC1 > 0) against pulp and albedo (PC1 < 0), while the second principal component (PC2) separated the pulp (PC2 < 0) and albedo (PC2 > 0) (Figure 2). The biplot in Figure 2A shows metabolites that are potentially significant in the discrimination of the parts based on contributions and reliability of the separation observed in the score scatter plot (Figures S7 and S8 supplementary material). The incidence of citric acid determined the distribution of the pulp on the bottom-left part of the plot, contributing to the higher activity in both DPPH• and ABTS•+ assays, while the radical scavenging activity of the albedo is related to the incidence of rutin, luteolin-O-rutinoside, and neerocitrin phenolic compounds, along with the limonoid isobacunoic acid. The rest of the phenolic compounds, limonoids, and the detected coumarins determined the discrimination of the peels on the right part of the plot. The incidence of compounds is highlighted in detail by the positive bars of the score contribution (Figure 2B).

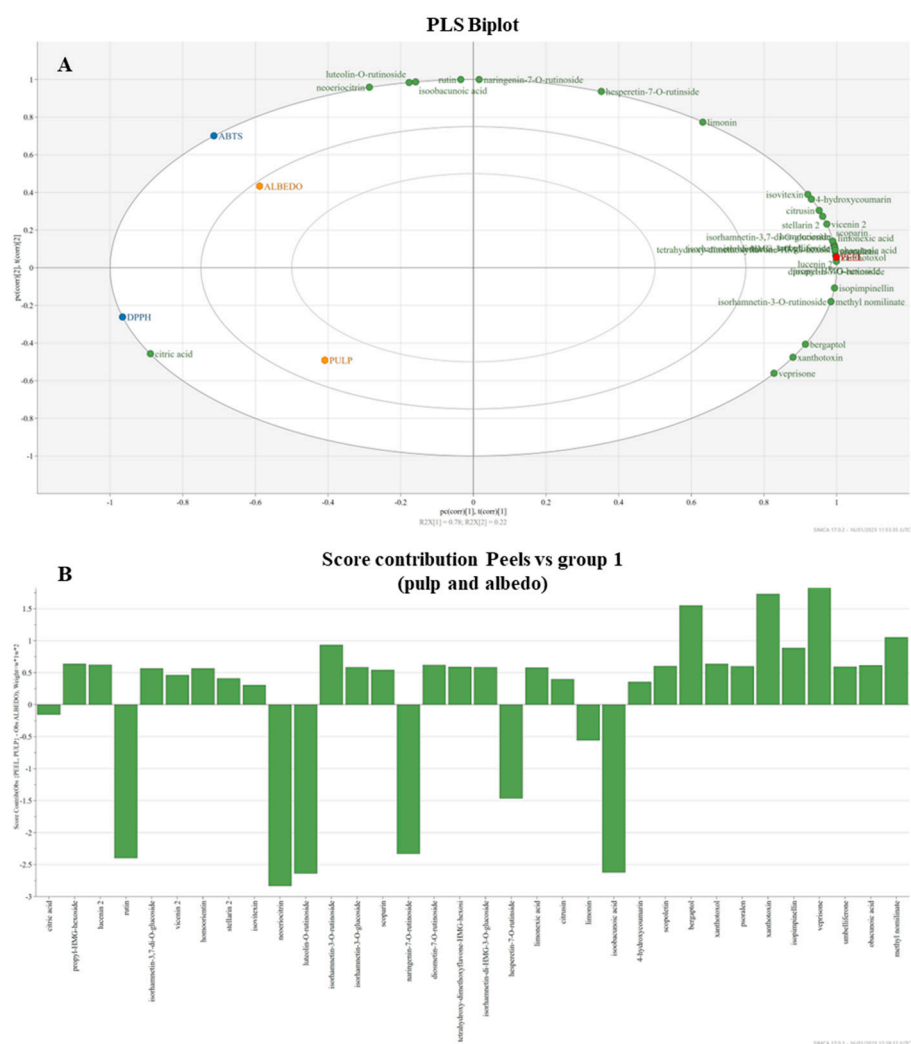


Figure 2. Biplot of PLS analysis performed on peels, pulp, and albedo for the identified non-volatile compounds (A). Contribution diagram of the constituents on the distribution of samples (B).

4. Conclusions

A comprehensive chemical investigation on VOCs and non-volatile constituents of Faustrime was performed by GC-MS and UHPLC-QTOF-MS/HRMS analysis. Monoterpenes and sesquiterpenes were the most abundant VOCs identified, describing a citronellal/limonene/linalyl acetate chemotype. Coumarins (60–66), along with C-glycoside flavonoids (75, 78–79, 86), limonoids (67–70, 93, 95), and HMG-glycoside flavonoids (89, 91), were reported for the first time in the species. In particular, MS spectra of compound 91 was described for the first time in this species and tentatively attributed to isorhamnetin-di-HMG-O-glycoside. The metabolomic description of constituents of PE, PU, AL, and SE was defined by PCA plots highlighting the relevant occurrence of α -bisabolol, 2-menthen-1-ol, and α -trans-bergamotol VOCs in the cluster of pulp and seeds, whereas the non-volatile compounds were particularly relevant in the peel. The spectrophotometric assays for DPPH \bullet and ABTS \bullet^+ radical scavenging capacity showed the higher activity of the edible pulp and albedo, usually considered as a by-product of the fruit. The PCA modeling defined the incidence of citric acid in the discrimination of pulp and phenolic compounds rutin, neeroiocitrin and luteolin-O-rutinoside in the albedo. The antioxidant potential of the peels was attributed to the investigated coumarins and phenolic compounds. The consistent data obtained in the complex workflow of the foodomic approach defined the metabolome of bioactive compounds in the Faustrime fruits as a source of high-value constituents for future application in products with health-promoting effects.

Supplementary Materials: The following supporting information can be downloaded at: <https://www.mdpi.com/article/10.3390/antiox12030565/s1>, Figure S1: GC-MS Profiles of PPAS parts n-hexane extracts. Figure S2: UPLC-HRMS profiles of PPAS parts chloroform extracts. Figure S3: UPLC-HRMS profiles of PPAS parts methanol/water (50% v/v) extracts. Figure S4: MS/HRMS spectra of compound 91. Figure S5: PCA Loading Plot. Figure S6: PCA Score Plot. Figure S7: PLS Loading Plot. Figure S8: PLS Score Plot. Table S1: Calibration curves for semi-quantitative analysis.

Author Contributions: Conceptualization, M.L. and L.C.; funding acquisition M.L. and P.B.; data curation C.C., S.P., S.C. and C.M.G.; formal analysis S.P., C.C., C.M.G., W.G.N. and S.C.; investigation, C.C. and S.P.; supervision, M.L., M.R., P.B. and L.C.; writing—original draft, L.C., M.R., P.B. and M.L. All authors have read and agreed to the published version of the manuscript.

Funding: Project funded under the National Recovery and Resilience Plan (NRRP), Mission 4. Component 2 Investment 1.4—Call for tender No. 3138 of 16 December 2021, rectified by Decree n.3175 of 18 December 2021 of Italian Ministry of University and Research funded by the European Union—NextGenerationEU; Award Number: Project code CN_00000033, Concession Decree No. 1034 of 17 June 2022. Adopted by the Italian Ministry of University and Research, CUP, H43C22000530001 Project title “National Biodiversity Future Center—NBFC”.

Institutional Review Board Statement: Not applicable.

Informed Consent Statement: Not applicable.

Data Availability Statement: The original contributions presented in this study are included in the article. Further inquiries can be directed to the corresponding author.

Conflicts of Interest: The authors declare no conflict of interest.

References

1. Delort, E.; Jaquier, A.; Decorzant, E.; Chapuis, C.; Casilli, A.; Frérot, E. Comparative Analysis of Three Australian Finger Lime (*Citrus australasica*) Cultivars: Identification of Unique Citrus Chemotypes and New Volatile Molecules. *Phytochemistry* **2015**, *109*, 111–124. [[CrossRef](#)] [[PubMed](#)]
2. Delort, E.; Jaquier, A. Novel Terpenyl Esters from Australian Finger Lime (*Citrus australasica*) Peel Extract. *Flavour. Fragr. J.* **2009**, *24*, 123–132. [[CrossRef](#)]
3. Dugo, P.; Mondello, L.; Zappia, G.; Bonaccorsi, I.; Cotroneo, A.; Russo, M.T. The Composition of the Volatile Fraction and the Enantiomeric Distribution of Five Volatile Components of Faustrime Oil (Monocitrus AustralaticaXfortunellasp.Xcitrus Urantifolia. *J. Essent. Oil Res.* **2004**, *16*, 328–333. [[CrossRef](#)]
4. Trozzi, A.; Verzera, A.; d’Alcontres, I.S. Constituents of the Cold-Pressed Oil of Faustrime, A Trigenic Hybrid of Monocitrus Australasica x Fortunella Sp. X Citrus Aurantifolia. *J. Essent. Oil Res.* **1993**, *5*, 97–100. [[CrossRef](#)]
5. Cozzolino, R.; Câmara, J.S.; Malorni, L.; Amato, G.; Cannavacciuolo, C.; Masullo, M.; Piacente, S. Comparative Volatilomic Profile of Three Finger Lime (*Citrus australasica*) Cultivars Based on Chemometrics Analysis of HS-SPME/GC-MS Data. *Molecules* **2022**, *27*, 7846. [[CrossRef](#)]
6. Campone, L.; Celano, R.; Rizzo, S.; Piccinelli, A.L.; Rastrelli, L.; Russo, M. Development of an Enriched Polyphenol (Natural Antioxidant) Extract from Orange Juice (*Citrus sinensis*) by Adsorption on Macroporous Resins. *J. Food Qual.* **2020**, *2020*, 1251975. [[CrossRef](#)]
7. Benavente-García, O.; Castillo, J. Update on Uses and Properties of Citrus Flavonoids: New Findings in Anticancer, Cardiovascular, and Anti-Inflammatory Activity. *J. Agric. Food Chem.* **2008**, *56*, 6185–6205. [[CrossRef](#)]
8. Alam, M.A.; Subhan, N.; Rahman, M.M.; Uddin, S.J.; Reza, H.M.; Sarker, S.D. Effect of Citrus Flavonoids, Naringin and Naringenin, on Metabolic Syndrome and Their Mechanisms of Action. *Adv. Nutr.* **2014**, *5*, 404–417. [[CrossRef](#)]
9. Cioni, E.; Migone, C.; Ascrizzi, R.; Muscatello, B.; de Leo, M.; Piras, A.M.; Zambito, Y.; Flamini, G.; Pistelli, L. Comparing Metabolomic and Essential Oil Fingerprints of Citrus Australasica F. Muell (*Finger lime*) Varieties and Their In Vitro Antioxidant Activity. *Antioxidants* **2022**, *11*, 2047. [[CrossRef](#)]
10. Celano, R.; Campone, L.; Pagano, I.; Carabetta, S.; di Sanzo, R.; Rastrelli, L.; Piccinelli, A.L.; Russo, M. Characterisation of Nutraceutical Compounds from Different Parts of Particular Species of Citrus Sinensis ‘Ovale Calabrese’ by UHPLC-UV-ESI-HRMS. *Nat. Prod. Res.* **2019**, *33*, 244–251. [[CrossRef](#)]
11. Galdani, R.; Cavalluzzi, M.M.; Lentini, G.; Habtemariam, S. The Chemistry and Pharmacology of Citrus Limonoids. *Molecules* **2016**, *21*, 1530. [[CrossRef](#)] [[PubMed](#)]
12. Lončar, M.; Jakovljević, M.; Šubarić, D.; Pavlič, M.; Služek, V.B.; Cindrić, I.; Molnar, M. Coumarins in Food and Methods of Their Determination. *Foods* **2020**, *9*, 645. [[CrossRef](#)] [[PubMed](#)]
13. Thakur, A.; Singla, R.; Jaitak, V. Coumarins as Anticancer Agents: A Review on Synthetic Strategies, Mechanism of Action and SAR Studies. *Eur. J. Med. Chem.* **2015**, *101*, 476–495. [[CrossRef](#)] [[PubMed](#)]

14. Balkir, P.; Kemahlioglu, K.; Yucel, U. Foodomics: A New Approach in Food Quality and Safety. *Trends Food Sci. Technol.* **2021**, *108*, 49–57. [[CrossRef](#)]
15. Guzowska, M.; Wasiak, W.; Wawrzyniak, R. Comparison of Extraction Techniques for the Determination of Volatile Organic Compounds in Liverwort Samples. *Molecules* **2022**, *27*, 2911. [[CrossRef](#)]
16. Cannavacciuolo, C.; Napolitano, A.; Heiss, E.H.; Dirsch, V.M.; Piacente, S. Portulaca Oleracea, a Rich Source of Polar Lipids: Chemical Profile by LC-ESI/LTQOrbitrap/MS/MSn and in Vitro Preliminary Anti-Inflammatory Activity. *Food Chem.* **2022**, *388*, 132968. [[CrossRef](#)]
17. Pagliari, S.; Cannavacciuolo, C.; Celano, R.; Carabetta, S.; Russo, M.; Labra, M.; Campone, L. Valorisation, Green Extraction Development, and Metabolomic Analysis of Wild Artichoke By-Product Using Pressurised Liquid Extraction UPLC–HRMS and Multivariate Data Analysis. *Molecules* **2022**, *27*, 7157. [[CrossRef](#)]
18. D’Urso, G.; Napolitano, A.; Cannavacciuolo, C.; Masullo, M.; Piacente, S. Okra Fruit: LC-ESI/LTQOrbitrap/MS/MS: Nbased Deep Insight on Polar Lipids and Specialized Metabolites with Evaluation of Anti-Oxidant and Anti-Hyperglycemic Activity. *Food Funct.* **2020**, *11*, 7856–7865. [[CrossRef](#)]
19. Biancolillo, A.; Bucci, R.; Magri, A.L.; Magri, A.D.; Marini, F. Data-Fusion for Multiplatform Characterization of an Italian Craft Beer Aimed at Its Authentication. *Anal. Chim. Acta* **2014**, *820*, 23–31. [[CrossRef](#)]
20. Tian, Q.; Schwartz, S.J. Mass Spectrometry and Tandem Mass Spectrometry of Citrus Limonoids. *Anal. Chem.* **2003**, *75*, 5451–5460. [[CrossRef](#)]
21. Kaanin-Boudraa, G.; Brahmi, F.; Wrona, M.; Nerín, C.; Moudache, M.; Mouhoubi, K.; Madani, K.; Boulekbache-Makhlouf, L. Response Surface Methodology and UPLC-QTOF-MSE Analysis of Phenolic Compounds from Grapefruit (*Citrus × Paradisi*) by-Products as Novel Ingredients for New Antioxidant Packaging. *LWT* **2021**, *151*, 112158. [[CrossRef](#)]
22. Zhang, J.; Xu, Y.; Ho, C.T.; Qiu, J.Q.; Qiu, X.H.; Huang, Z.H.; Zhang, L.; Xu, W. Phytochemical Profile of Tibetan Native Fruit “Medog Lemon” and Its Comparison with Other Cultivated Species in China. *Food Chem.* **2022**, *372*, 131255. [[CrossRef](#)] [[PubMed](#)]
23. Guo, P.; Pang, W.; Zhao, X.; Chen, X.; Zhang, Y.; Zhao, Q.; Jiao, B. A Rapid UPLC-QqQ-MS/MS Method for Targeted Screening and Quantitative Analysis of Secondary Metabolites in Satsuma Mandarin. *Eur. Food Res. Technol.* **2021**, *247*, 1725–1736. [[CrossRef](#)]
24. Su, B.; Tian, J.; Liu, M.; Wang, K.; Yang, W.; Ning, J.; Li, Y.; Zheng, G. Analysis of the Chemical Components of Pomelo Peels (*Citrus grandis* [L.] Osbeck) from Different Cultivars by Using Supercritical CO₂ Fluid Extraction and Ultra-High-Performance Liquid Chromatography-Tandem Mass Spectrometry. *J. Sep. Sci.* **2022**, *45*, 3031–3042. [[CrossRef](#)]
25. Shi, Y.S.; Zhang, Y.; Li, H.T.; Wu, C.H.; El-Seedi, H.R.; Ye, W.K.; Wang, Z.W.; Li, C.B.; Zhang, X.F.; Kai, G.Y. Limonoids from Citrus: Chemistry, Anti-Tumor Potential, and Other Bioactivities. *J. Funct. Foods* **2020**, *75*, 104213. [[CrossRef](#)]
26. Gao, P.; Wang, L.; Zhao, L.; Lu, Y.; Zeng, K.; Zhao, M.; Jiang, Y.; Tu, P.; Guo, X. Rapid Identification, Isolation, and Evaluation on Anti-Neuroinflammatory Activity of Limonoids Derivatives from the Root Bark of *Dictamnus Dasycarpus*. *J. Pharm. Biomed. Anal.* **2021**, *200*, 114079. [[CrossRef](#)]
27. Su, Y.; Tao, L.; Zhang, X.; Sheng, X.; Li, Q.; Fei, W.; Yin, T.; Kang, A.; Aa, J.; Wang, G. Non-Targeted Characteristic Filter Analysis Combined with in Silico Prediction Strategies to Identify the Chemical Components and in Vivo Metabolites of Dalitong Granules by UPLC-Q-TOF/MS/MS. *J. Pharm. Biomed. Anal.* **2023**, *222*, 115086. [[CrossRef](#)]
28. Li, X.; Yang, Y.; Zhu, Y.; Ben, A.; Qi, J. A Novel Strategy for Discriminating Different Cultivation and Screening Odor and Taste Flavor Compounds in Xinhui Tangerine Peel Using E-Nose, E-Tongue, and Chemometrics. *Food Chem.* **2022**, *384*, 132519. [[CrossRef](#)]
29. Wang, Y.; Ji, S.; Zang, W.; Wang, N.; Cao, J.; Li, X.; Sun, C. Identification of Phenolic Compounds from a Unique Citrus Species, Finger Lime (*Citrus australasica*) and Their Inhibition of LPS-Induced NO-Releasing in BV-2 cell Line. *Food Chem. Toxicol.* **2019**, *129*, 54–63. [[CrossRef](#)]
30. Goh, R.M.V.; Pua, A.; Ee, K.H.; Huang, Y.; Liu, S.Q.; Lassabliere, B.; Yu, B. Investigation of Changes in Non-Traditional Indices of Maturation in Navel Orange Peel and Juice Using GC–MS and LC-QTOF/MS. *Food Res. Int.* **2021**, *148*, 110607. [[CrossRef](#)]
31. Barreca, D.; Gattuso, G.; Laganà, G.; Leuzzi, U.; Bellocco, E. C- and O-Glycosyl Flavonoids in Sanguinello and Tarocco Blood Orange (*Citrus sinensis* (L.) Osbeck) Juice: Identification and Influence on Antioxidant Properties and Acetylcholinesterase Activity. *Food Chem.* **2016**, *196*, 619–627. [[CrossRef](#)] [[PubMed](#)]
32. Lim, V.; Gorji, S.G.; Daygon, V.D.; Fitzgerald, M. Untargeted and Targeted Metabolomic Profiling of Australian Indigenous Fruits. *Metabolites* **2020**, *10*, 114. [[CrossRef](#)] [[PubMed](#)]
33. Aznar, R.; Rodríguez-pérez, C.; Rai, D.K. Comprehensive Characterization and Quantification of Antioxidant Compounds in Finger Lime (*Citrus australasica* L.) by HPLC-QToF-MS and UPLC-MS/MS. *Appl. Sci.* **2022**, *12*, 1712. [[CrossRef](#)]
34. Barreca, D.; Bellocco, E.; Leuzzi, U.; Gattuso, G. *Flavonoid C-Glycosides in Citrus Juices from Southern Italy: Distribution and Influence on the Antioxidant Activity*; American Chemical Society: Washington, DC, USA, 2014. [[CrossRef](#)]

35. Fu, Q.; Zhang, C.; Lin, Z.; Sun, H.; Liang, Y.; Jiang, H.; Song, Z.; Wang, H.; Chen, S. Rapid Screening and Identification of Compounds with DNA-Binding Activity from Folium Citri Reticulatae Using on-Line HPLC–DAD–MSn Coupled with a Post Column Fluorescence Detection System. *Food Chem.* **2016**, *192*, 250–259. [[CrossRef](#)]
36. Cuevas, F.J.; Pereira-Caro, G.; Moreno-Rojas, J.M.; Muñoz-Redondo, J.M.; Ruiz-Moreno, M.J. Assessment of Premium Organic Orange Juices Authenticity Using HPLC-HR-MS and HS-SPME-GC-MS Combining Data Fusion and Chemometrics. *Food Control* **2017**, *82*, 203–211. [[CrossRef](#)]

Disclaimer/Publisher’s Note: The statements, opinions and data contained in all publications are solely those of the individual author(s) and contributor(s) and not of MDPI and/or the editor(s). MDPI and/or the editor(s) disclaim responsibility for any injury to people or property resulting from any ideas, methods, instructions or products referred to in the content.